

# Co-Combustion Characteristics of Inferior Coal and Biomass Blends in an Oxygen-Enriched Atmosphere

Ge Pu,\* Weilin Zhu, Huping Zhou, Qiang Lei, Zhengren Zhang, and Jianjun Liu

Combustion characteristics and thermal dynamic characteristics of blends of inferior coal and core plywood under different oxygen-enriched atmospheres were investigated using thermogravimetric (TG) analysis. According to the results, with increasing oxygen concentration, TG and DTG curves tended to move to a lower temperature region. The comprehensive combustion characteristic index  $S_M$  was first proposed in this work, suggesting that the enriched oxygen concentration can significantly improve the combustion conditions. Apparent activation energies were also put into the calculation and analysis, which showed that the apparent activation energy increases with an increasing oxygen concentration. The factor  $F_c (A p_{o_2}^x / \beta)$  was defined for the first time, and it was found that  $F_c$  can represent the temperature at which combustion can proceed under the same blend ratio condition.

*Keywords:* Oxygen-enrichment; Co-combustion; Comprehensive combustion characteristic index

*Contact information:* Key Laboratory of Low-grade Energy Utilization Technologies and Systems, Chongqing University, Ministry of Education of PRC, 400030, China;

\* *Corresponding author:* puge@cqu.edu.cn; Tel.: +86-23-6510-2107; fax: +86-23-6510-2107

## INTRODUCTION

Oxygen-enriched combustion is a method of burning in which the oxygen content in a combustion-supporting gas is higher than that of ambient air. Compared with the conventional combustion method, oxygen-enriched combustion can lower the fuel ignition point and make the burning start in advance. Oxygen-enriched combustion also requires a lesser amount of combustion-supporting gas, which reduces the loss of heat and raises the concentration of CO<sub>2</sub> in the exhaust gas. Furthermore, the combustion efficiency is enhanced and carbon dioxide capture is advanced.

Intrigued by the advantages that oxygen-enriched combustion presents, researchers all over the world have performed a lot of investigations on the combustion of coal and biomass in an oxygen-enriched atmosphere. Investigations of oxygen-enriched combustion of coal (Folgueras *et al.* 2003; Luo *et al.* 2009; Varol *et al.* 2010; Qin *et al.* 2012; Yuzbasi and Selçuk 2012) mainly have focused on the influence of oxygen concentration, coal type, and grain size on combustion characteristics (*i.e.*, ignition temperature, temperature of max DTG, the temperature of burnout, and synthetic combustion factor). Studies on oxygen-enriched combustion of biomass have mainly focused on how different kinds of biomass (*i.e.*, municipal wastes) (Xiao *et al.* 2009), wood (Kastanaki *et al.* 2002; Fang *et al.* 2006; Liu *et al.* 2009), agricultural wastes (Yu *et al.* 2008), and microalgae (Chen *et al.* 2011) perform under an oxygen-enriched atmosphere. There also have been some studies on coal-char and coal/biomass blends (Gani *et al.* 2005; Idris *et al.* 2012; Parshetti *et al.* 2013).

Many of the previous experiments and trials have studied oxygen-enriched combustion on coal or biomass; however, less attention has been given to co-combustion of coal and biomass blends, especially with inferior coal and core plywood gathered from building decoration plate wastes. It is under this scenario that combustion characteristics and thermal dynamic characteristics of blends of inferior coal with core plywood in an oxygen-enriched atmosphere were studied using thermogravimetric analysis (TGA) in this work. Such studies may be of importance for cost-effective utilization of inferior coal as well as for the comprehensive utilization of municipal wastes and carbon dioxide emission reduction.

## EXPERIMENTAL

### Materials

The inferior coal used in this study was collected from a coal mine near Chongqing City, China. The biomass used was core plywood, which was derived from the decoration plate wastes of a metropolitan building. The samples of inferior coal and core plywood blends were prepared by crushing, drying, blending, and sieving to particle sizes of 120 to 150  $\mu\text{m}$ . The blend ratios (M) in the experiments were 10%, 20%, and 30% (core plywood mass/total mass).

### Methods

The experiments were carried out with a STA409PC (NETZSCH, Germany) type thermal gravity analyzer with differential thermal analysis (DTA) support and a cylindrical alumina crucible.

In the experiments, 10 mg of each sample was heated to 1000  $^{\circ}\text{C}$  from room temperature at a constant heating rate of 25  $^{\circ}\text{C}/\text{min}$  under different oxygen-enriched concentrations (20%, 30%, and 40%) at a flow rate of 100 mL/min. These different oxygen concentrations were achieved by mixing oxygen and nitrogen gas together. The TG and DTG data of each experiment were obtained from the data acquisition unit. The TG and DTG curves were drawn from these data and were used to assess the combustion characteristics of the samples under different oxygen-enriched atmospheres.

The proximate analysis of the inferior coal and core plywood was carried out according to ASTM E870-82, and the results shown in Table 1. It is known from the ultimate analysis of experimental samples that the inferior coal is high in ash ( $A_{\text{ad}} = 28.85\%$ ), but low in volatile matter ( $V_{\text{ad}} = 16.97\%$ ), which is unfavorable for combustion. This disadvantage of the inferior coal, however, can be compensated by the rich volatile matter in biomass ( $V_{\text{ad}} = 83.79\%$ ).

**Table 1.** Proximate Analysis of Samples (wt%, Ad)

| Samples       | Moisture <sub>ad</sub> | Volatile <sub>ad</sub> | Ash <sub>ad</sub> | Fixed carbon <sub>ad</sub> |
|---------------|------------------------|------------------------|-------------------|----------------------------|
| Inferior coal | 0.84                   | 16.97                  | 28.85             | 53.34                      |
| Core plywood  | 4.13                   | 83.79                  | 2.71              | 13.69                      |

Ad: as determined basis

## RESULTS AND DISCUSSION

### TG and DTG Analysis

Figure 1 shows the TG and DTG curves under different oxygen concentrations ( $\varphi = 20\%$ ,  $30\%$ , and  $40\%$ ) and different blend ratios (core plywood mass/total mass:  $10\%$ ,  $20\%$ , and  $30\%$ ). According to the TGA and TG results, three regions and two peaks were observed. The first region, which is due to the moisture and low boiling point of the organic matters in the sample, is called the water evaporation region (around  $40$  to  $150$  °C). The experimental samples were dried and kept in a drying oven; hence there was not much moisture volatilized. The other two regions are an oxidative pyrolysis (around  $150$  to  $400$  °C) and a char combustion region (around  $400$  to  $850$  °C). After moisture evaporation, two major mass loss peaks were observed in the DTG curves. The first peak is due to the release of volatiles and their combustion, and the second peak is due to the combustion of the fixed carbon. The first peak is combined with the second peak and it is like a shoulder to the second peak, which represents the release of volatiles in the inferior coal and the combustion of fixed carbon in the biomass.

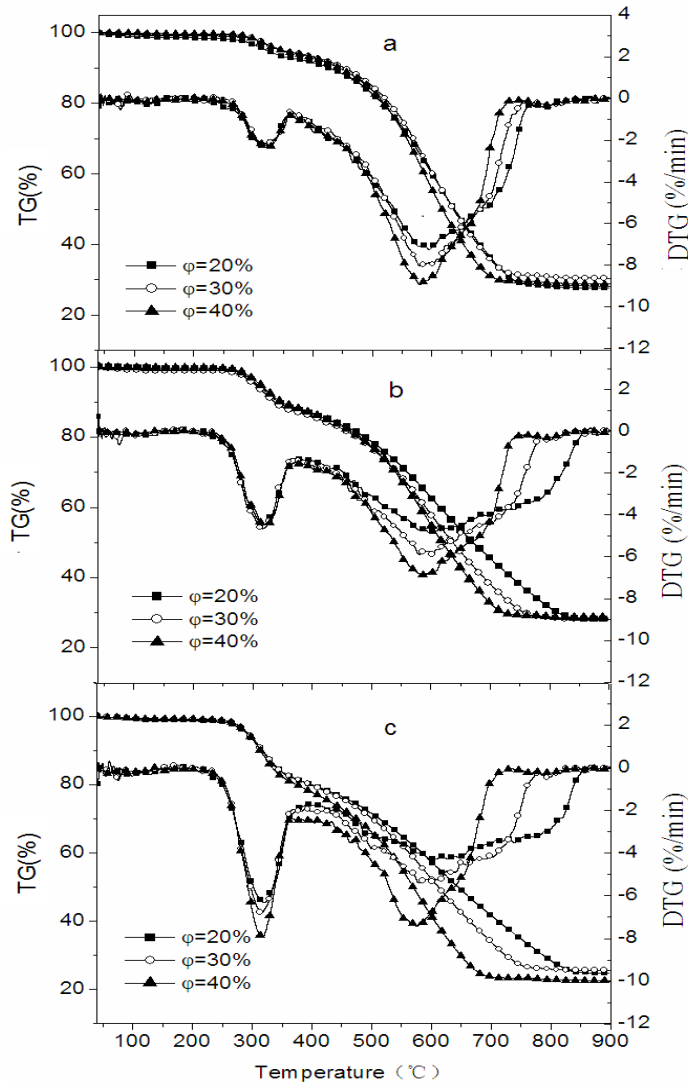


**Fig. 1.** DG and DTG curves of mixtures for  $\varphi=20\%$ ,  $30\%$ , and  $40\%$ : (a) blend ratio  $M=10\%$ , (b) blend ratio  $M=20\%$ , and (c) blend ratio  $M=30\%$

It also can be seen in Fig. 1 that for the lower blend ratios ( $M=10\%$  and  $20\%$ ), the oxygen concentration  $\phi$  had little impact on the release of volatiles, as indicated by the similar TG curves in the volatile release region (around  $150$  to  $400$  °C) of the samples. For the blend ratio  $M$  of  $30\%$ , the maximum mass loss rate ( $-6.31056\%$ ,  $-6.979985\%$ ,  $-7.91374\%$  respectively) of the sample increased with increasing oxygen concentration, as observed by the DTG curves; the volatiles also were released quickly.

In the fixed carbon combustion region (around  $400$  to  $850$  °C), however, the oxygen concentration  $\phi$  and blend ratio  $M$  played a positive role. At the same blend ratio, the TG curves and DTG curves shifted to the lower temperature region as the oxygen concentration increased and the maximum mass loss rate increased, indicating favorable conditions for the combustion process of fixed carbon under an oxygen-enriched atmosphere.

### Characteristics of Ignition and Burnout Temperature

As shown in Fig. 2, a DT-DTG plot (Gil *et al.* 2010) was used to define the ignition temperature of the biomass  $T_{i1}$ , the ignition temperature of the inferior coal  $T_{i2}$ , and the burnout temperature  $T_b$ .

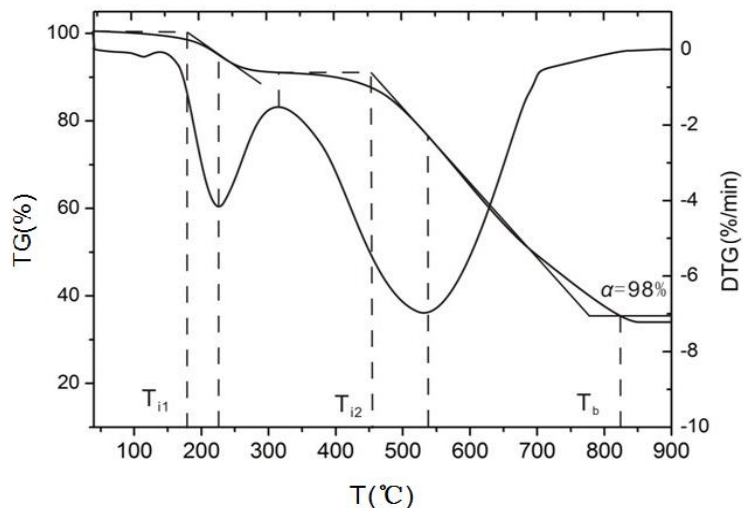


**Fig. 2.** Ignition temperatures and burnout temperature

The ignition temperature of the biomass  $T_{i1}$  and the ignition temperature of the inferior coal  $T_{i2}$  under different mixing ratios  $M$  and oxygen concentrations  $\phi$  are given in Table 2. The ignition temperatures of the biomass and inferior coal decreased slightly with the increasing oxygen concentration. For the biomass, its ignition temperature maintained at about  $280$  °C, compared to  $470$  °C for the inferior coal.

The variations of peak temperature ( $T_{max}$ ) and maximum mass loss rate ( $DTG_{max}$ ) with different mixing ratios and oxygen concentrations in the fixed carbon combustion region are given in Table 2, where  $T_{max}$  represents the temperature at which the rate of mass loss is at a maximum.

As shown in Table 2, the peak temperature ( $T_{max}$ ) decreased when the oxygen concentration  $\phi$  increased from  $20\%$  to  $40\%$ , while the maximum mass loss rate ( $DTG_{max}$ ) increased. The  $T_{max}$  of these three samples (mixing ratio  $M=10\%$ ,  $20\%$ , and  $30\%$ ) dropped  $15$  °C,  $10$  °C, and  $22$  °C, respectively, and  $DTG_{max}$  increased  $1.74\%$ ,  $2.01\%$ , and  $3.11\%$ , respectively.

**Table 2.** Kinetic Parameters of the Samples with Variations of  $M$  (Mixing Ratio) and  $\phi$  (Oxygen Concentrations)

| $M$ | $\phi$ | $T_{i1}$<br>(°C) | $T_{i2}$<br>(°C) | $T_{max}$<br>(°C) | $DTG_{max}$<br>(%/min) | $T_b$<br>(°C) | $E$<br>(kJ/mol) | Factor $F_c$<br>(Pa/K) |
|-----|--------|------------------|------------------|-------------------|------------------------|---------------|-----------------|------------------------|
| 10% | 20%    | 288.39           | 490.98           | 595.62            | -7.18                  | 746.42        | 56.30           | 16.46                  |
|     | 30%    | 287.41           | 490.34           | 580.40            | -8.03                  | 731.20        | 61.33           | 37.27                  |
|     | 40%    | 279.52           | 486.42           | 580.54            | -8.92                  | 708.14        | 63.37           | 60.15                  |
| 20% | 20%    | 283.20           | 474.65           | 597.22            | -4.88                  | 818.42        | 38.67           | 0.83                   |
|     | 30%    | 281.99           | 472.77           | 579.60            | -5.89                  | 760.00        | 40.16           | 1.23                   |
|     | 40%    | 278.84           | 472.00           | 587.34            | -6.89                  | 721.74        | 46.03           | 3.53                   |
| 30% | 20%    | 280.94           | 467.93           | 597.22            | -4.32                  | 820.40        | 27.82           | 0.14                   |
|     | 30%    | 277.54           | 466.34           | 579.60            | -5.40                  | 750.40        | 37.83           | 0.90                   |
|     | 40%    | 277.33           | 467.12           | 575.34            | -7.43                  | 688.94        | 46.45           | 5.31                   |

$T_{i1}$ : ignition temperature of the biomass;  $T_{i2}$ : ignition temperature of the inferior coal;  
 $T_{max}$ : variation of peak temperature;  $DTG_{max}$ : maximum mass loss rate  
 $T_b$ : burnout temperature;  $E$ : activation energy; Factor  $F_c$ :  $A\phi xO_2/\beta$  was defined

The burnout temperature  $T_b$  under different mixing ratios  $M$  and different oxygen concentrations  $\phi$  are listed in Table 2. It shows that the higher the oxygen concentration  $\phi$ , the lower the burnout temperature. This observation was more pronounced with the 30% mixing ratio, evidenced by a 132 °C drop in burnout temperature compared to a 38 °C drop with a mixing ratio of 10%, which strongly demonstrates that the addition of biomass to coal will promote the combustion of the coal. It can be also concluded that the oxygen-enriched atmosphere makes the combustion process of the blend proceed at a lower temperature, which reduces the heat waste.

### Analysis of Comprehensive Combustion Characteristics

In related works, a combustion characteristic index  $S$  was used to evaluate the comprehensive behavior of the combustion of biomass or coal (Wu *et al.* 2008) according to Eq. 1,

$$S = \frac{(dw/dt)_{max} (dw/dt)_{mean}}{T_i^2 T_b} \quad (1)$$

where  $(dw/dt)_{max}$  and  $(dw/dt)_{mean}$  are the maximum and average mass loss rates, respectively, and  $T_i$  and  $T_b$  are the ignition and burnout temperatures, respectively.

The combustion characteristic index  $S$ , however, is not applicable for biomass/coal blends, especially when the characteristic of the biomass and coal has great variation. Therefore, the synthetic combustion index of blends  $S_M$  was proposed in this study in order to evaluate the combustion behavior of the blends and eliminate the effects caused by different blend ratios, and computed as follows:

$$S_M = \frac{\sum_{j=1,2} (dw_j/dt)_{max}}{2 (dw/dt)_{mean}} \frac{2}{\left[ \frac{\sum_{j=1,2} T_{ij}}{2} \right]^2 T_b} \quad (2)$$

The first item in the numerator is the arithmetical average value of the maximum mass loss rates in the volatile release region and in the fixed carbon combustion region, respectively. The second item is the average mass loss rate value from the ignition temperature of the biomass  $T_{i1}$  to burnout temperature  $T_b$ . The first item in the denominator is the square of the arithmetical average value of  $T_{i1}$  and  $T_{i2}$ . The comprehensive combustion characteristic index  $S_M$  of the biomass/coal blends under different oxygen concentrations  $\varphi$  are shown in Fig. 3.

As can be observed in Fig. 3, the value of  $S_M$  increased as the oxygen concentration  $\varphi$  increased, indicating that the oxygen-enriched atmosphere enhanced the combustion behavior of the blends. In addition, the slopes of the fitting curves grew synchronously with oxygen concentration. When the blend ratio  $M$  was 30%, the  $S_M$  line had a maximum increasing trend.

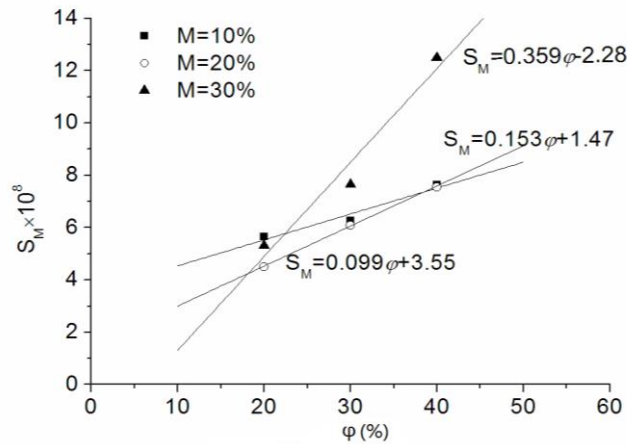


Fig. 3. Synthetic combustion index of blends  $S_M$  with different  $O_2$  concentrations  $\varphi$

### Activation Energy Calculation and Analysis

A non-isothermal kinetic equation was adopted (Hu *et al.* 2001) as follows,

$$\frac{d\alpha}{dT} = \frac{1}{\beta} k(T, p_{O_2}) f(\alpha) \quad (3)$$

where  $T$  is the thermodynamic temperature, and  $p_{O_2}$  is the oxygen partial pressure.  $\alpha$  is the extent of conversion or weight loss fraction at time  $\tau$  and is calculated as:  $\alpha = (w - w_l) / (w_0 - w_l)$ , where  $w_0$  is the initial mass of the blends sample before combustion;  $w$  is the mass at time  $\tau$ , and  $w_l$  is the final mass that remained at the end of combustion.

Taking the impact of oxygen concentration into consideration and the Arrhenius Law,  $k$  is defined as follows (Kastanaki and Vamvuka 2006; Aracil *et al.* 2007):

$$k = A \exp(-E / RT) p_{O_2}^x \quad (4)$$

where  $A$  is the frequency factor,  $E$  represents activation energy,  $R$  is the universal gas constant, and  $x$  is constant. Inserting Eq. 4 into Eq. 3, one obtains,

$$\frac{d\alpha}{dT} = \frac{1}{\beta} A \exp(-E/RT) f(\alpha) p_{O_2}^x \quad (5)$$

Taking the logarithm of Eq. 3 and transposing,

$$\ln\left(\frac{d\alpha/dT}{f(\alpha)}\right) = \ln\left(\frac{A}{\beta} p_{O_2}^x\right) + \frac{-E}{R} \frac{1}{T} \quad (6)$$

Usually,  $f(\alpha)$  is illustrated as  $f(\alpha) = (1 - \alpha)^n$  in dynamic experimental methods; therefore, Eq. 6 finally is written as:

$$\ln\left(\frac{d\alpha/dT}{(1-\alpha)^n}\right) = \ln\left(\frac{A}{\beta} p_{O_2}^x\right) + \frac{-E}{R} \frac{1}{T} \quad (7)$$

From Eq. 7, the activation energy  $E$  in the fixed carbon combustion region and correlation coefficient  $r$  can be calculated by plotting  $\ln(Ap_{O_2}^x/\beta)$  versus  $1/T$ . Calculated results are given in Table 2, from which it can be seen that all the correlation coefficient  $r$  values are at least 0.983, indicating that the model is a good fit for the data.

As seen in Table 2, at the same mixing ratio condition, the activation energy within the fixed carbon combustion region exhibited an ascending trend with oxygen concentration, which is consistent with the features of coal or biomass (Fang *et al.* 2006; Yu *et al.* 2008). When the blend ratio  $M$  was 10%, the activation energy calculated at a 10% oxygen concentration was 56.30 kJ/mol and it steadily increased until a 30% oxygen concentration to a value of 63.37 kJ/mol. This can be explained by the hypothesis that coal consists of substances whose activation energy is distributed from low to high. As discussed earlier, an oxygen-enriched atmosphere allows combustion to take place at a lower temperature; therefore, when the oxygen concentration increases, the substance with the higher activation energy will react at a lower temperature. Thus, the activation energy of the samples increased with the increasing oxygen concentration at the same mixing ratio.

Under the same oxygen concentration conditions, however, the activation energy of the samples decreased as the blend ratio  $M$  increased (Table 2). The reason relies on the fundamental fact that the activation energy of biomass is lower than that of coal within the same temperature region. Consequently, the activation energy of the samples dropped while the blend ratio  $M$  increased.

### Promoting Effect of Oxygen Concentration

After observation and analysis of Eq. 5,  $Ap_{O_2}^x/\beta$  was defined as factor  $F_c$  in this work. It is found that factor  $F_c$  can represent the promotion effect of oxygen concentration on the co-combustion of biomass/coal blends, because frequency factor  $A$  reflects the molecular internal thermal mobility;  $p_{O_2}^x$  is the oxygen partial pressure and the higher oxygen concentration will enhance the combustion process as discussed above.  $\beta$  is the heating rate and its value is expected to be small for full combustion. Consequently, the higher factor  $F_c$ , the greater effect on promoting mixed combustion of biomass/coal blends efficiency.

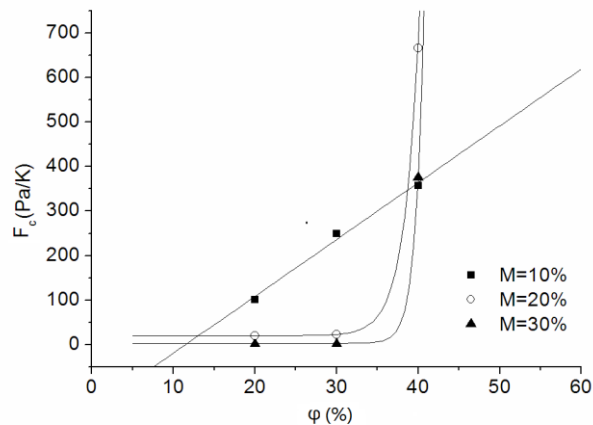


**Fig. 4.** Variations of FC in fixed carbon combustion region

Variations of  $F_c$  in the fixed carbon combustion region are plotted in Fig. 4. Oxygen concentration had a great impact on the  $F_c$  value. For the same blend ratio, the  $F_c$  value calculated at a 40% oxygen concentration was larger than that calculated at 20% and 30% oxygen concentrations, indicating that the oxygen-enriched atmosphere could promote the co-combustion of the biomass/coal blends.

### Compensation Effect of Factor $F_c$

The plot of  $\ln(F_c)$  versus  $E$  is represented in Fig. 5, where factor  $F_c$  is the value calculated at the different mixing ratios and oxygen concentrations. Through fitting, the linear equation is as follows:

$$\ln(F_c) = 0.167E - 6.48 \quad (8)$$

According to the fitting results, the correlation coefficient  $r$  reached up to 0.99139, indicating that the factor  $F_c$  has a linearization compensation effect to the activation energy of the blended samples. As activation energy increases, more heat energy must be absorbed by blends; however, since factor  $F_c$  represents the degree of promotion effect to the combustion,  $F_c$  increases simultaneously with activation energy to provide the energy needed.

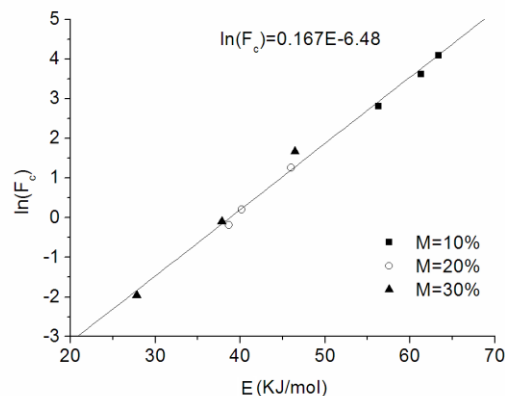


**Fig. 5.** Relation between  $F_c$  and apparent activation energy

## CONCLUSIONS

1. Based on the present work, it was concluded that a higher oxygen concentration results in a greater mass loss rate and lower peak temperature ( $T_{\max}$ ). In addition, the burnout temperature decreases under oxygen-enriched atmosphere conditions, so the combustion process shifts to a lower temperature region, which reduces heat waste and favors the combustion of biomass/coal blends.
2. The comprehensive combustion characteristic index SM was first proposed, and the comprehensive combustion characteristic of blended samples can be significantly improved by increasing the oxygen concentration, especially with a blend ratio of 30%.
3. At the same oxygen concentration, the activation energy within the fixed carbon combustion region decreases with increasing blend ratio, which is useful to accelerate reaction rate. This occurs because an oxygen-enriched atmosphere makes the combustion process proceed at a lower temperature.
4. Factor  $F_c$  can represent the positive promotion effect of oxygen concentration on the co-combustion of biomass/coal blends. Factor  $F_c$  also has a linearization compensation effect on activation energy ( $E$ ) of blended samples.

## ACKNOWLEDGMENTS

The authors gratefully acknowledge financial support from the Chongqing Science & Technology Commission (Project No: CSTC, 2013jjB90003).

## REFERENCES CITED

- Aracil, I., Font, R., Conesa, J. A., and Fullana, A. (2007). "TG-MS analysis of the thermo-oxidative decomposition of polychloroprene," *Journal of Analytical and Applied Pyrolysis* 79(1-2), 327-336. DOI: 10.1016/j.jaap.2006.12.027
- Chen, C., Ma, X., and Liu, K. (2011). "Thermogravimetric analysis of microalgae combustion under different oxygen supply concentrations," *Applied Energy* 88(9), 3189-3196. DOI: 10.1016/j.apenergy.2011.03.003
- Fang, M. X., Shen, D. K., Li, Y. X., Yu, Z. Y., and Cen, K. F. (2006). "Kinetic study on pyrolysis and combustion of wood under different oxygen concentrations by using TG-FTIR analysis," *Journal of Analytical and Applied Pyrolysis* 77(1), 22-27. DOI: 10.1016/j.jaap.2005.12.010
- Folgueras, M. B., Díaz, R. M., Xiberta, J., Jorge, X., and Ismael, P. (2003). "Thermogravimetric analysis of the co-combustion of coal and sewage sludge," *Fuel* 82(15), 2051-2055. DOI: 10.1016/S0016-2361(03)00161-3
- Gani, A., Morishita, K., Nishikawa, K., and Naruse, K. (2005). "Characteristics of co-combustion of low-rank coal with biomass," *Energy & Fuels* 19(4), 1652-1659. DOI: 10.1021/ef049728h
- Gil, M. V., Casal, D., Pevida, C., Pis, J. J., and Rubiera, F. (2010). "Thermal behaviour and kinetics of coal/biomass blends during co-combustion," *Bioresource Technology* 101(14), 5601-5608. DOI: 10.1016/j.biortech.2010.02.008
- Hu, R. Z., and Shi, Q. Z. (2001). *Kinetics of Thermal Analysis*, Science Press, Beijing.

- Hu, Y. Q., Nikzat, H., Nawata, M., Kobayashi, N., and Hasatani, M. (2001). "The characteristics of coal-char oxidation under high partial pressure of oxygen," *Fuel* 80(14), 2111-2116. DOI: 10.1016/S0016-2361(01)00086-2
- Idris, S., Rahman, N. A., and Ismail, K. (2012). "Combustion characteristics of Malaysian oil palm biomass, sub-bituminous coal and their respective blends via thermogravimetric analysis (TGA)," *Bioresour Technol* 123(1), 581-591. DOI: 10.1016/j.biortech.2012.07.065
- Kastanaki, E., and Vamvuka, D. A. (2006). "Comparative reactivity and kinetic study on the combustion of coal-biomass char blends," *Fuel* 85(9), 1186-1193. DOI: 10.1016/j.fuel.2005.11.004
- Kastanaki, E., Vamvuka, D., Grammelis, P., and Kakaras, E. (2002). "Thermogravimetric studies of the behavior of lignite-biomass blends during devolatilization," *Fuel Processing Technology* 77-78, 159-166. DOI: 10.1016/S0378-3820(02)00049-8
- Liu, G. H., Ma, X. Q., and Yu, Z. (2009). "Experimental and kinetic modeling of oxygen-enriched air combustion of municipal solid waste," *Waste Management* 29(2), 792-796. DOI: 10.1016/j.wasman.2008.06.010
- Luo, S. Y., Xiao B., Hu, Z. Q., Liu, S. M., and Guan, Y. M. (2009). "Experimental study on oxygen-enriched combustion of biomass micro fuel," *Energy* 34(11), 1880-1884. DOI: 10.1016/j.energy.2009.07.036
- Qin, Y., Liu, W., Yang, C., Fan, Z. Z., Wang, L. L., and Jia, G. W. (2012). "Experimental study on oxygen consumption rate of residual coal in goaf," *Safety Science* 50(4), 787-791. DOI: 10.1016/j.ssci.2011.08.033
- Varol, M., Atımtay, A. T., Bay, B., and Olgun, H. (2010). "Investigation of co-combustion characteristics of low quality lignite coals and biomass with thermogravimetric analysis," *Thermochimica Acta* 510(1), 195-201. DOI: 10.1016/j.tca.2010.07.014
- Wu, X. Y., Yu, G. R., Chen, X. C., Wang, Y. H., Liu, C. J., and Sun, W. (2008). "Intrinsic kinetics of reoxidation reaction for a multicomponent molybdate catalyst by thermal analysis method," *Catalysis Communications* 10(7), 1066-1069. DOI: 10.1016/j.catcom.2008.12.056
- Xiao, H., Ma, X., and Lai, Z. (2009). "Isoconversional kinetic analysis of co-combustion of sewage sludge with straw and coal," *Applied Energy* 86(9), 1741-1745. DOI: 10.1016/j.apenergy.2008.11.016
- Yu, Z. S., Ma, X. Q., and Liu, A. (2008). "Kinetic studies on catalytic combustion of rice and wheat straw under air-and oxygen-enriched atmospheres, by using thermogravimetric analysis," *Biomass and Bioenergy* 32(11), 1046-1055. DOI: 10.1016/j.biombioe.2008.02.001
- Yuzbasi, N. S., and Selçuk, N. (2012). "Air and oxy-fuel combustion behaviour of petcoke/lignite blends," *Fuel* 92(1), 137-144. DOI: 10.1016/j.ssci.2011.08.033

Article submitted: October 21, 2014; Peer review completed: December 17, 2014;  
Revised version received: December 28, 2014; Accepted: January 12, 2015; Published:  
January 16, 2015.